MDPI

Article

Assessment and Optimization of Residential Microgrid Reliability Using Genetic and Ant Colony Algorithms

Eliseo Zarate-Perez [1,2,*] and Rafael Sebastian [2,*]

1 Department of Research, Innovation and Sustainability, Universidad Privada del Norte (UPN), Av. Alfredo Mendiola 6062, Los Olivos 15314, Peru
2 Department of Electrical, Electronic and Control Engineering (DIEEC), Universidad Nacional de Educación a Distancia (UNED), Juan del Rosal, 12, 28040 Madrid, Spain
* Correspondence: eliseo.zarate@upn.edu.pe or ezarate9@alumno.uned.es (E.Z.-P.); rsebastian@ieec.uned.es (R.S.); Tel.: +51-1-6259600 (E.Z.-P.); +34-913986000 (R.S.)

Abstract: The variability of renewable energy sources, storage limitations, and fluctuations in residential demand affect the reliability of sustainable energy systems, resulting in energy deficits and the risk of service interruptions. Given this situation, the objective of this study is to diagnose and optimize the reliability of a residential microgrid based on photovoltaic and wind power generation and battery energy storage systems (BESSs). To this end, genetic algorithms (GAs) and ant colony optimization (ACO) are used to evaluate the performance of the system using metrics such as loss of load probability (LOLP), loss of supply probability (LPSP), and availability. The test system consists of a 3.25 kW photovoltaic (PV) system, a 1 kW wind turbine, and a 3 kWh battery. The evaluation is performed using Python-based simulations with real consumption, solar irradiation, and wind speed data to assess reliability under different optimization strategies. The initial diagnosis shows limitations in the reliability of the system with an availability of 77% and high values of LOLP (22.7%) and LPSP (26.6%). Optimization using metaheuristic algorithms significantly improves these indicators, reducing LOLP to 11% and LPSP to 16.4%, and increasing availability to 89%. Furthermore, optimization achieves a better balance between generation and consumption, especially in periods of low demand, and the ACO manages to distribute wind and photovoltaic generation more efficiently. In conclusion, the use of metaheuristics is an effective strategy for improving the reliability and efficiency of autonomous microgrids, optimizing the energy balance and operating costs.

Keywords: renewable energy; microgrid reliability; genetic algorithm (GA); ant colony optimization (ACO); battery energy storage system (BESS); loss of load probability (LOLP); loss of supply probability (LPSP); metaheuristic optimization; energy management; stochastic modeling

1. Introduction

The current energy crisis is driven not only by dependence on fossil fuels, but also by the urgent need to transition to a sustainable and decarbonized energy system. According to the 2030 Agenda, it is essential to change the energy paradigm and promote the use of non-polluting renewable energy sources, as well as to significantly improve efficiency and generation capacity. In this context, the challenge posed by fossil fuels, which is addressed in SDG 7 (Affordable and Clean Energy), is part of the energy transition concept, which aims to replace the current fossil fuel-based model with a sustainable system that aims to maintain ecological balance and ensure a cleaner energy future [1]. In recent

years, the use and development of microgrids have increased significantly, becoming an efficient solution for promoting the consumption of renewable energy and improving the reliability of electrical systems. A microgrid is a localized energy system that integrates distributed generation, energy storage, controllable loads, and, in some cases, microturbines. It can be connected to the main grid or operate in isolation, providing resiliency and optimizing energy management [2]. These networks integrate various energy sources, such as renewable generation, storage systems, loads, and microturbines, with the goal of optimizing energy management and making complementary use of available resources [3].

Solar photovoltaic and wind power have gained prominence in power generation due to their abundance and technological advances. Their adoption has grown rapidly, driving the energy transition and reducing carbon emissions in electrical systems [4]. However, the intermittent nature of these renewable sources poses challenges to the stability of supply. To counteract this variability, energy storage systems (ESSs), especially battery energy storage systems (BESSs), have been proposed to balance electricity supply and demand. Their implementation has improved the reliability and sustainability of the electrical system by ensuring a more stable flow of energy [5]. Based on these advances, residential microgrids have emerged as an efficient solution for integrating renewable energy generation with battery storage. These infrastructures operate independently or are connected to existing power grids, increasing system resilience and facilitating the transition to a more sustainable and secure energy model [6].

However, the inherent variability of these sources, limited storage capacity, and the seasonal and hourly variability of residential demand continue to compromise the reliability of the sustainable energy system, creating periods of energy deficit and affecting the availability of supply. Therefore, their intermittency poses challenges to the economic stability and reliability of the supply [7].

Consequently, one of the main challenges in the design and operation of microgrids is to ensure an optimal balance between energy generation, storage, and consumption. To achieve this, it is essential to minimize the loss of load probability (LOLP) and optimize the implementation and operating costs [8]. In addition, the operation of microgrids requires continuous diagnosis and optimization due to various factors affecting their performance. Among the main factors affecting the efficiency and stability of a microgrid are changes in energy demand patterns, which may be due to population growth, adoption of new technologies, and seasonal variations [9].

Similarly, fluctuations in renewable energy generation due to changes in solar radiation and wind speed can affect the stability of the system. Another critical aspect is the degradation of storage systems, which reduces the autonomy of the microgrid and affects its operational reliability [10]. In addition, technological advances and the development of new optimization strategies offer the opportunity to improve efficiency and reduce costs, but they also require constant updating and adaptation of existing systems. Traditional configurations may not be sufficient to cope with these fluctuations, so advanced optimization strategies must be implemented to diagnose and determine the optimal capacity of the microgrid [9].

Traditional microgrid sizing techniques typically include the peak load method, which sizes generation and storage according to the expected maximum demand, with the goal of ensuring supply during critical conditions, but with the risk of oversizing and high costs [11]. The average load method, which is based on average consumption, reduces costs compared to the previous method but may compromise reliability in the face of peak demand. The energy balance method seeks a balance between production and consumption over a given period, optimizing the use of renewable energy, although it may require conservative sizing of backup systems. The code and standard method ensure

compliance with regulatory requirements but are not always optimal from an economic and operational standpoint. Finally, the reliability analysis method uses metrics such as LOLP and Expected Energy Not Supplied (EENS) to improve system reliability, although its implementation is complex and costly.

On the other hand, different optimization algorithms are used [11], which are divided into deterministic, metaheuristic, and those based on artificial intelligence and machine learning. Deterministic algorithms, such as linear programming (LP), nonlinear programming (NLP), dynamic programming (DP), and mixed integer linear programming (MILP), provide exact solutions when accurate data are available, although they can be computationally expensive for problems with multiple variables and constraints [12]. Algorithms based on artificial intelligence and machine learning, such as artificial neural networks (ANN) and reinforcement learning (RL), can predict consumption and generation patterns with high accuracy [13]. However, they require large amounts of data for training and validation, which can limit their applicability [14]. Metaheuristic algorithms have proven to be effective tools in power system optimization because they can find optimal solutions to complex and nonlinear problems.

Among them, genetic algorithm (GA) and ant colony optimization (ACO) stand out for their applicability to microgrid sizing [15]. GA uses principles of biological evolution to optimize the distribution of energy resources, while ACO models the behavior of ants to find optimal routes in network planning. Both algorithms improve system reliability by optimizing resource allocation and minimizing service interruptions.

In [16], a robust formulation of multi-objective two-stage optimization with stochastic modeling is proposed to improve the operation of active distribution systems with demand response. While the stochastic approach accounts for uncertainty, it does not account for real-time adaptability. However, the study by [17] proposes an optimization approach for renewable microgrids using GA and Model Predictive Control (MPC). A system consisting of photovoltaic and wind generation, fuel cells, and battery storage was optimized, considering power flow constraints and battery state of charge. The main objective was to minimize the Cost of Energy (COE), the loss of supply probability (LPSP), and the Net Present Cost to guarantee the technical and economic viability of the system.

For their part, ref. [5] propose an optimization approach for the sizing of renewable energy systems with battery storage and fuel cell electrolyzers. They use Particle Swarm Optimization (PSO) and GAs to optimize solar and wind generation capacity, storage, and hydrogen conversion, considering the nonlinearity of the problem. The results show a 33–35% cost reduction and a 16–20% increase in demand coverage compared to hydrogen-only systems.

In another approach, ref. [18] uses an optimization algorithm based on multilayer ant colonies to improve energy planning in autonomous microgrids. This algorithm manages to reduce energy consumption by 5% compared to PSO. In [19], a dynamic programming algorithm based on ACO is developed to reduce costs and improve operational reliability. By optimizing the loading and unloading of storage systems using LCOE as a reference, it is possible to reduce the total cost of generation and increase the profitability of the system.

However, the studies do not directly use reliability metrics to determine the optimal sizing and configuration of hybrid microgrids that combine photovoltaic (PV), wind, and BESS generation. To address this, GA is used for its efficiency in solving complex nonlinear optimization problems, while ACO is selected for its adaptability in optimizing operational scheduling. Both could contribute to a given problem from different perspectives. As a result, the following research gaps were identified:

- The lack of integration of reliability metrics (LOLP, EENS) in the optimal sizing and configuration of hybrid microgrids.

- Limitations of AI-based optimization algorithms due to the need for large amounts of data for training and validation.
- Existing methods cannot adapt to real-time variations in demand and generation.
- Proposed optimization techniques have limited scalability and have not been validated with real data.

In response to this need, the objective is to diagnose and optimize the reliability of a residential microgrid based on PV, wind, and BESS using GA and ACO, evaluating its performance in terms of probability of load loss, availability, and cost. The contributions are as follows:

- It incorporates reliability metrics into the optimization process to improve the stability of the microgrid.
- It develops a hybrid optimization model for renewable microgrids that considers multiple energy sources and storage technologies and uses real data.
- It also introduces adaptive optimization strategies to cope with fluctuations in demand and renewable energy generation.
- It also improves economic viability by minimizing costs and ensuring optimal system performance.

Section 2 describes the methodology used, including the modeling of the microgrid and the implementation of the optimization algorithms. Then, Section 3 presents the results obtained and a comparative analysis between the evaluated configurations. Finally, Section 4 discusses the implications of the results and draws conclusions about the effectiveness of metaheuristic algorithms in optimizing residential microgrids.

2. Materials and Methods

Figure 1 shows the methodology used to model the residential microgrid. First, photovoltaic and wind generation are evaluated. Next, the BESS is modeled, evaluating its state of charge (SOC) and operating limits. Similarly, a power balance is performed, analyzing total demand, available energy supply, and energy not supplied (ENS). Next, in the reliability phase, failures are modeled using the Mean Time to Failures (MTTFs), and metrics such as LOLP, loss of supply probability (LPSP), and system availability are evaluated. Finally, optimization is performed using GA and ACO, for which fitness functions, operational constraints, and convergence criteria are defined to improve the reliability and efficiency of the system.

Figure 2 shows the architecture of a hybrid energy generation and storage system installed in a residential building to evaluate and analyze its performance. The system integrates a 1 kW wind turbine, a 3 kWh BESS, and a 3.30 kW photovoltaic system. The energy generated by these sources is managed through a direct current (DC) bus, where it is regulated by alternating current (AC) and direct current (DC) inverters, allowing it to be used in the electrical loads of the house. In the event of an energy deficit, the system is designed to receive energy from the distribution system without returning any surplus to it.

2.1. Renewable Energy Generation Modeling

To model renewable energy generation and energy balance, real data on estimated residential demand are combined with environmental variables such as solar irradiance and wind speed. These parameters provide an accurate estimate of the system's energy production and ability to meet demand, as shown in Figure 3. D(t) was collected with a smart meter and then extracted for a computer, while the meteorological data were extracted from the NRL [20].
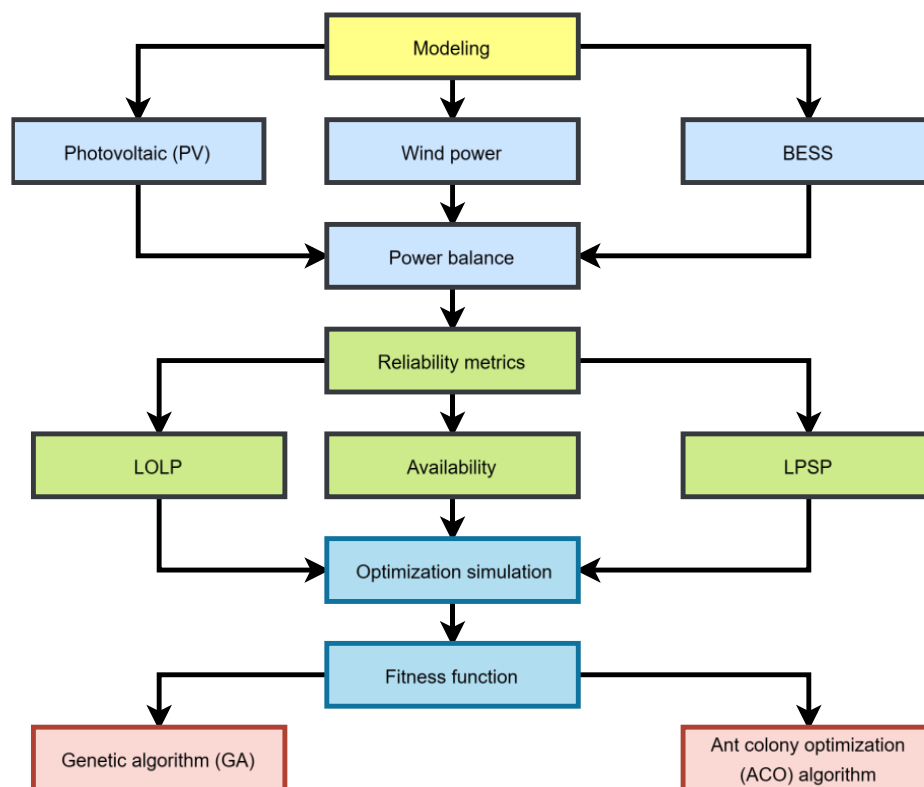
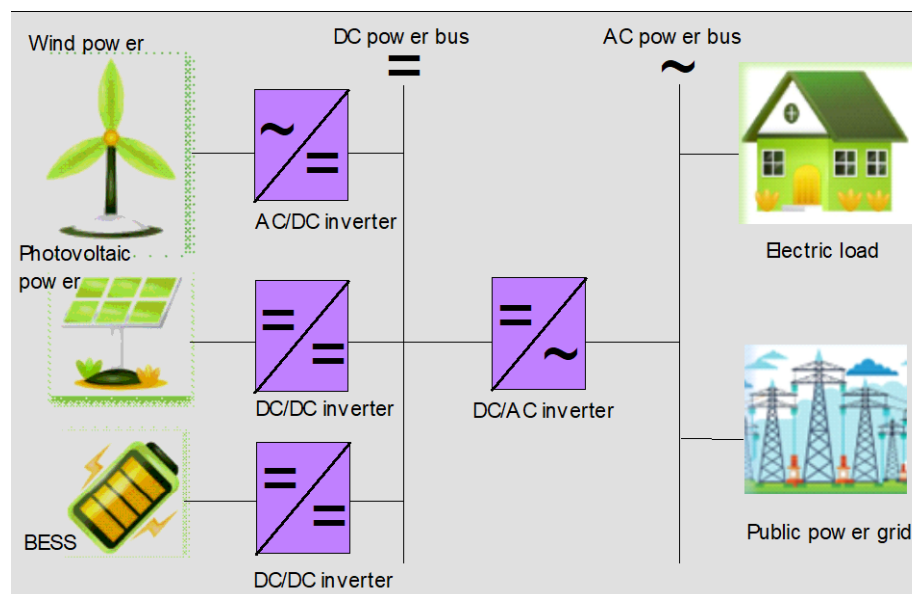**Figure 1.** Methodological sequence used.

Figure 2. Structure of the evaluated residential microgrid.

Table 1 shows the main parameters of the generation components of the photovoltaic, wind, and BESSs, such as power, efficiency, and operating limits. In addition, their descriptions, reference values, and units are detailed to perform the modeling and simulation of the residential hybrid microgrid.
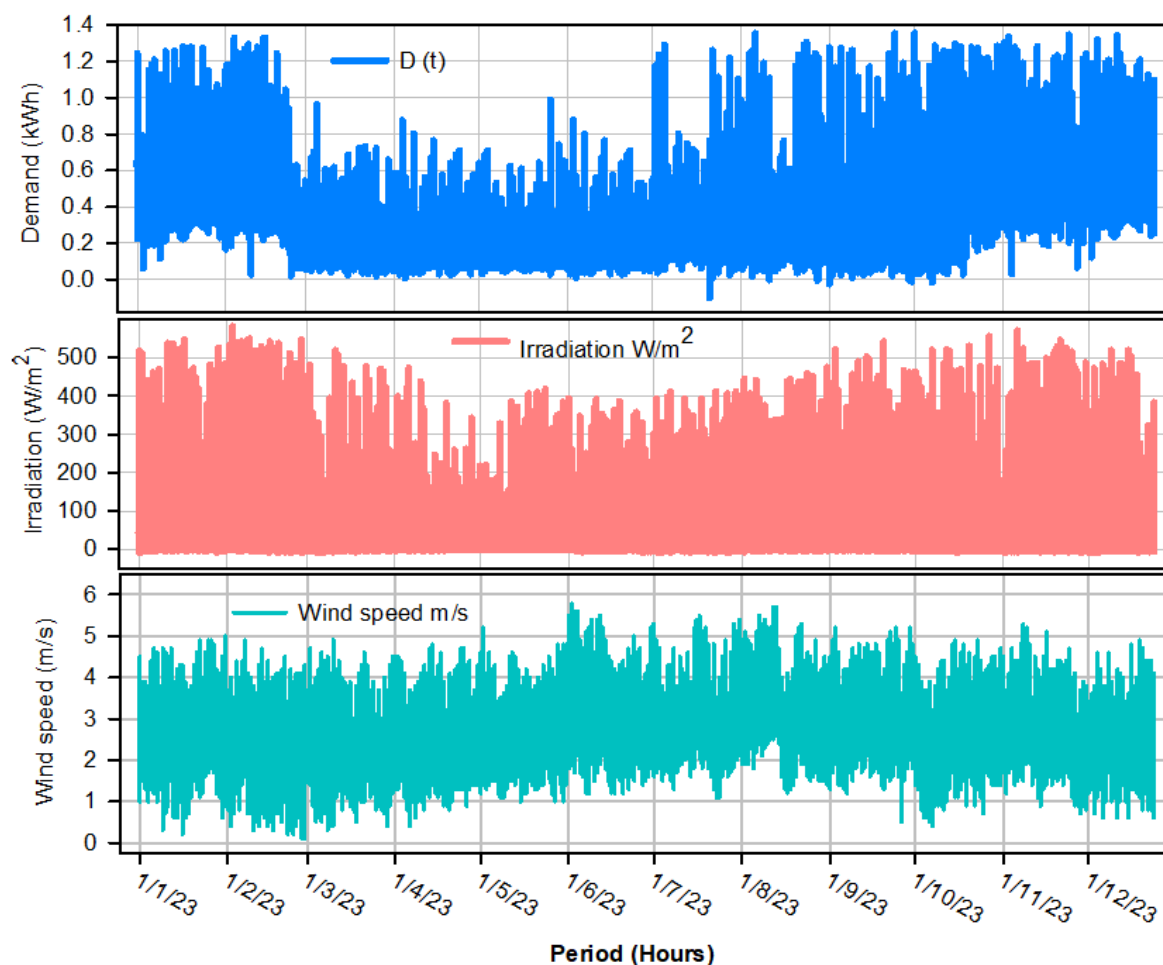
Figure 3. Data used for the analysis of renewable production and energy balance.

Table 1. Parameters for photovoltaic, wind power generation, and battery energy storage systems (BESSs).

Category	Variable/Parameter	Description	Values	Units
Photovoltaic Generation	$G_{hour}(t)$	Solar irradiance	-	W/m^2
	P_max	Maximum power	550	W
	A	Effective area of solar panels	2.582	m^2
	η_{PV}	Efficiency of PV system	21	%
Wind Power Generation	V(t)	Wind speed	-	m/s
	ρ	Air density	1225	kg/m^3
	V_{cut-in}	Minimum turbine operating speed	2.5	m/s
	$V_{cut-out}$	Maximum turbine operating speed	45	m/s
	V_{rated}	Nominal turbine speed	12	m/s
	P_{rated}	Nominal turbine power	1	kW
	A_{rotor}	Effective rotor area	2.83	m^2
State of Charge (SOC)	C_p	Power coefficient	-	Dimensionless
	$P_{chg(t)}$	Battery charge power	-	kW
	$P_{dchg(t)}$	Battery discharge power	-	kW
	C_{bess}	Total battery capacity	3 (Base)	kWh
	η_c	Charge efficiency	0.9	Dimensionless
	η_d	Discharge efficiency	0.9	Dimensionless
BESS	SOC_{min}	Minimum allowed SOC	0.2	Dimensionless
	SOC_{max}	Maximum allowed SOC	0.9	Dimensionless

2.1.1. Photovoltaic (PV) Power Generation

Photovoltaic energy production is modeled using Equation (1), which uses solar irradiance, the effective area of the panels, the efficiency of the photovoltaic system, and the total number of solar panels [21].

$$P_{PV}(t) = G_{hour}(t) \cdot A_{panel} \cdot \eta_{PV} \cdot N_{pv} \tag{1}$$

where $G_{hour}(t)$ is the solar irradiance in W/m^2 integrated over time t.

A_{panel} is the effective area of the solar panels (in m^2).

η_{PV} is the efficiency of the PV system, according to the manufacturer Tensite, which is 21%.

N_{PV} is the total number of photovoltaic panels.

The total energy produced by the photovoltaic panels (E_{PV}) in one period is calculated according to Equation (2).

$$E_{PV} = \sum_{t=1}^{T} P_{PV}(t) \tag{2}$$

2.1.2. Wind Power Generation

The power generated ($P_{wind,unit}(t)$) by a wind turbine is modeled by its power curve according to Equation (3) [22].

$$P_{wind,\,unit}(t) = \begin{cases} 0, & if \quad V(t) < V_{cut\text{-}in} \ o \ V(t) > V_{cut\text{-}out} \\ P_{rated}, & if \quad V_{rated} \leq V(t) \leq V_{cut\text{-}out} \\ 0.5 \cdot \ \rho * A_{rotor} \ \cdot C_p \cdot \ V(t)^3, & if \quad V_{cut\text{-}in} \leq V(t) < V_{rated} \end{cases} \tag{3}$$

where $V(t)$ is the wind speed in m/s at time t.

$V_{cut\text{-}in}$ and $V_{cut\text{-}out}$ are the minimum and maximum operating speeds of the wind turbine.

P_{rated} is the rated power of the turbine in kilowatts (kW).

ρ is the density of air in kg/m^3.

A_{rotor} is the rotor area in square meters.

C_p is the power coefficient, which is a dimensionless parameter. It represents the fraction of the kinetic energy of the wind that a wind turbine can convert into mechanical energy.

To find the total power generated ($P_{wind}(t)$) by a given number of wind turbines at time t, Equation (4) is used. Where N_{wt} is the number of turbines in operation.

$$P_{wind}(t) = N_{wt} \cdot P_{wind,\,unit}(t) \tag{4}$$

In this way, the energy generated by the turbines in a period (E_{wind}) is expressed by Equation (5).

$$E_{wind} = \sum_{t=1}^{T} P_{wind}(t) \tag{5}$$

2.1.3. Calculating the Total Energy Produced

In this way, the total power generated ($P_{gen}(t)$) in the system is the sum of both contributions and is expressed by Equation (6).

$$P_{gent}(t) = P_{pv}(t) + P_{wind}(t) \tag{6}$$

Therefore, the total energy produced in T periods is shown in Equation (7).

$$E_{gent} = \sum_{t=1}^{T} P_{gent}(t) \tag{7}$$

2.2. Storage System Modeling (BESS)

2.2.1. State of Charge (SOC) Calculation

SOC is a parameter that indicates the state of charge of the battery at a given time. It measures the energy stored in the battery in relation to its total capacity and is expressed in Equation (8) [23].

$$SOC_{(t+1)} = SOC_t + \frac{\eta_c \cdot P_{chg}(t) - \frac{P_{dchg}(t)}{n_d}}{C_{bess}} \tag{8}$$

where $SOC_{(t+1)}$ is the state of charge at time t + 1 (a dimensionless value between 0 and 1).

$SOC_{(t)}$ is the initial state of charge at time t.

η_c is the charge efficiency (dimensionless, between 0 and 1, with a value of 0.9).

η_d is the discharge efficiency (dimensionless, between 0 and 1; in this case, it is taken as 0.9).

$P_{chg}(t)$ is the battery charge power at time t in kW.

$P_{dchg}(t)$ is the battery discharge power at time t in kW.

C_{bess} is the total battery capacity in kWh.

2.2.2. SOC Operating Limits

Equation (9) states that the battery back-up level should not fall below a minimum limit nor exceed a maximum limit that ensures the safe and efficient operation of the energy storage system.

$$SOC_{min} \leq SOC(t) \leq SOC_{max} \tag{9}$$

A minimum SOC of 20% is set to avoid deep discharge, which could damage the battery. Similarly, the maximum SOC is 90% to avoid overcharging and extend battery life.

2.3. Power Balance

2.3.1. Assessment of the Overall Demand

The total hourly residential energy demand (D(t)) is the amount of electricity consumed in the dwelling during each hour of the day, expressed in kilovolt-hours (kWh). This demand varies according to the use of electrical appliances, lighting, and air conditioning, as well as seasonal factors and user habits, as shown in Figure 2.

2.3.2. Energy Supply Calculation

The objective of energy supply is to ensure a continuous and stable flow of electricity to meet consumer demand. When generation plus storage meets demand, as shown in Equation (10), the relationship is fulfilled [24].

$$P_{(sup)} = D(t) \tag{10}$$

2.3.3. Calculation of Energy Not Supplied (ENS)

If generation plus storage does not meet demand, the energy not supplied (ENS) is shown in Equation (11) [24].

$$ENS(t) = D(t) - \left(P_{pv}(t) + P_{wind}(t) + P_{bess}(t)\right) \tag{11}$$

Therefore, the total energy not delivered (TENS) is shown in Equation (12).

$$EENS = \sum_{t=1}^{T} ENS(t) \tag{12}$$

Expected Energy Not Supplied (EENS) is a metric used to analyze the reliability of electrical systems and represents the energy that a system cannot deliver to consumers due to outages, generation constraints, or distribution system limitations.

2.3.4. Failure Modeling and Reliability

For renewable energy systems, Mean Time to Failure (MTTF) is defined as the average time without generation, i.e., the probability that a system will not generate electricity at a given time. In this sense, the probability density function of the time without generation can be modeled by a Weibull distribution according to Equation (13) [25].

$$f(t) = \frac{\beta}{\eta} \left(\frac{t}{\eta}\right)^{\beta-1} e^{-\left(\frac{t}{\eta}\right)^{\beta}} \tag{13}$$

where η is the characteristic of a lifetime.

β is the shape parameter.

2.3.5. Assessing System Availability

System Availability (A) is an indicator that reflects the proportion of time a renewable energy generation system is operating and producing electricity relative to the total assessment time. This measure includes both periods of active generation and intervals of non-generation due to factors such as environmental conditions, scheduled maintenance, or grid constraints, and is shown in Equation (14) [26].

$$A = \frac{MTTF}{MTTF + MTTR} \tag{14}$$

While MTTR in conventional systems measures the speed with which a failure is resolved, in renewable energy it captures periods of no generation, whether caused by outages, maintenance, or natural conditions.

2.4. Reliability Metrics

2.4.1. Calculate Loss of Load Probability (LOLP)

The LOLP measures the probability that the microgrid will experience an energy shortage in each period, as shown in Equation (15). It is a value between 0 and 1, with a LOLP close to 0 indicating that the microgrid can almost always meet demand, while a high LOLP indicates that the microgrid frequently experiences periods of insufficient generation [27].

$$LOLP = \frac{Hours \ with \ ENS > 0}{Total \ Hours} \tag{15}$$

2.4.2. Loss of Power Supply Probability (LPSP)

The LPSP is an indicator that measures the amount of unmet energy demand in an electrical system, especially in microgrids with intermittent renewable resources, as shown in Equation (16) [28].

$$LPSP = \frac{\sum_{t=1}^{T} ENS(t)}{\sum_{t=1}^{T} D(t)} \tag{16}$$

2.4.3. Calculating the "Availability" of the System

The availability of an electrical system represents the probability that the microgrid can meet the demand at a given time. It is calculated as the complement of the LOLP according to Equation (17) [29].

$$Availability = 1 - LOLP \tag{17}$$

2.5. Optimization Simulation

The objective is to optimize the design of a hybrid microgrid with photovoltaic (VPN), wind (NWT), and energy storage (BESScap) generation to minimize energy deficit and cost and maximize reliability and efficiency.

2.5.1. Definition of Fitness Function

The fitness function (f_f) is an evaluation criterion used to measure the quality of different configurations of an energy system, considering several performance factors. This function is particularly useful for optimizing microgrids or renewable energy generation systems, as shown in Equation (18) [30].

$$f_f = w_1 \cdot \left(1 - \frac{\sum_{t=1}^{T} ENS(t)}{\sum_{t=1}^{T} D(t)} \right) + w_2 \cdot n_{syst} - w_3 \cdot \frac{\sum_{t=1}^{T} E_{exc}(t)}{\sum_{t=1}^{T} P_{gen}(t)} - w_4 \cdot \frac{C_{total}}{C_{max}} \tag{18}$$

where ENS(t) is the energy not supplied at time t.

D(t) is the total energy demand at time t.

η_{syst} is the system efficiency.

$E_{exc}(t)$ is the excess energy not used at time t.

$P_{gen}(t)$ is the total energy produced at t, including both technologies.

C_{total} is the total cost of the system.

C_{max} is the maximum allowed cost.

w_1, w_2, w_3 and w_4 are the weights assigned to each criterion.

2.5.2. Assessment of Operational Constraints

Operational constraints define the limits and conditions under which an energy storage and delivery system can operate. These constraints are determined by three main factors: the storage capacity constraint (Equation (19)), the loading and unloading constraint (Equation (20)), and the energy delivery constraint (Equation (21)).

$$E_{bat,min} \leq E_{bat}(t+1) \leq E_{bat,\,max} \tag{19}$$

$$\eta_g \cdot E_{exc}(t) \leq BESS_{cap} - E_{bat}(t) \tag{20}$$

$$E_{supp}(t) \leq E_{reg}(t) \tag{21}$$

2.6. Implementation of Genetic Algorithm (GA)

2.6.1. Initialization and Population Generation

The initialization process of the GA is carried out by generating an initial population with random configurations of the parameters VPN, NWT, and BESS$_{cap}$, ensuring that they are within the predefined limits [30]:

$2 \leq$ VPN $\leq 20 \rightarrow$ number of solar panels (550 W each).

$1 \leq$ NWT $\leq 2 \rightarrow$ number of wind turbines (1000 W each).

$1 \leq$ BESS$_{cap} \leq 10 \rightarrow$ capacity of the battery storage system (kWh).

This procedure guarantees diversity in the initial population and allows efficient exploration of the search space within the given bounds.

2.6.2. Fitness Evaluation and Selection

The purpose of this procedure is to perform an exhaustive evaluation of everyone involved. For this purpose, a rigorous calculation of the fitness function (f_f) is implemented. This function allows to precisely quantify the quality of each solution within the search space, thus determining its performance with respect to the specific problem. Mathematically, this function is defined by Equation (22) [31].

$$F_x = fitness_x \tag{22}$$

In this context, F(x) represents the fitness value of individual x, calculated according to the established objectives (reliability, efficiency, cost, wasted energy), with the aim of minimizing or maximizing, depending on the case of everyone.

In the next phase of the process, the tournament technique is used to select the best individuals. The tournament is a probabilistic model that allows for the random selection and evaluation of k individuals from a given population, selecting the most suitable (Xbest), as shown in Equation (23) [31].

$$X_{best} = \frac{\arg max}{i \in S} F(X_i) \tag{23}$$

In the context of the tournament, the variable S represents the group of participating individuals made up of k elements. This increase in the probability of selecting solutions with high F(x) occurs without completely excluding optimal solutions, thus guaranteeing the preservation of diversity.

2.6.3. Crossing and Mutation

In the field of genetics, hybridization and mutation are fundamental processes in the reproduction and diversification of species.

In this context, crossing represents the integration of two parental solutions (p1, p2) to produce offspring. Mathematically, this process can be described by Equation (24) [31].

$$\begin{aligned}
c_1 &= \alpha p_1 + (1 - \alpha)p_2 \\
c_2 &= \alpha p_2 + (1 - \alpha)p_1
\end{aligned} \tag{24}$$

where $\alpha \in [0, 1]$ and is a factor that controls the mixing of the features.

c_1 and c_2 are the values generated because of this combination.

2.6.4. Stop Criteria

The mutation is implemented with the aim of introducing an element of randomness that allows for a systematic exploration of the search space. This modification is modeled by Equation (25) [31].

$$x' = x + \Delta \tag{25}$$

where x is defined as the original individual.

On the other hand, $\Delta \sim N(0, \sigma^2)$ represents a random (normal Gaussian) perturbation that subtly modifies x.

The population is then replaced by the fittest individuals (x_{elite}) according to the function F(x). The following population can be included by applying Equation (26) [31].

$$P_{next} = P_{elite} \cup P_{new} \tag{26}$$

where P_{elite} is the optimal fraction of current solutions.

P_{new} are the new individuals generated by crossbreeding and mutation.

Finally, the stopping criterion is implemented when there is no significant improvement or when the maximum number of generations is reached, as shown in Equation (27) [31].

$$
\begin{gathered}
\textit{Insignificant improvements}: \textit{if} \left| F_{best}^{(t)} - F_{best}^{(t-1)} \right| < \epsilon \textit{ during k generations} \\
\textit{Maximum generations}: t \geq t_{max}
\end{gathered}
\tag{27}
$$

2.7. Implementation of Ant Colony Optimization Algorithm (ACO)

2.7.1. Construction of Solutions

In the model proposed by ACO, the heuristic parameter η_{ij} is an important element in the decision-making process of the ants during the construction of solutions. This heuristic is intrinsically linked to the costs or values associated with the potential options between two nodes, i and j, as illustrated in Equation (28) [32].

$$
\eta_{ij} = \frac{1}{1 + f_{ij}}
\tag{28}
$$

where f_{ij} represents the value or cost associated with the option between nodes i and j. In this context, the weight of the f_{ij} heuristic influences how the ants make decisions, favoring optimal solutions.

2.7.2. Pheromone Deposition, Evaporation, and Algorithm Convergence

Once the construction of their solution is complete, the ants deposit pheromones on the paths used, where the amount of pheromone deposited is an indicator of the quality of the solution. High-quality solutions, defined as those with low f_ij (according to the weighting efficiency criterion), contribute to the updating of pheromones, thus strengthening the optimal paths for future generations of ants. This process ensures that the ants continue to select these paths, leading to a continuous improvement of the solution over time. Pheromone updating is performed using Equation (29) [33].

$$
\tau_{ij}(t + 1) = (1 - \rho) \cdot \tau_{ij}(t) + \Delta\tau_{ij}(t)
\tag{29}
$$

where $\tau_{ij}(t)$ represents the amount of pheromone present on the path between nodes i and j at time t.

ρ corresponds to the evaporation factor, which is in the interval $0 < \rho < 1$.

$\Delta\tau_{ij}(t)$ denotes the amount of pheromone deposited by the ants on the path $i \rightarrow j$ and is generally inversely related to the fixed cost, but for example, $\Delta\tau_{ij}(t) = 1/f_{ij}$.

This pheromone update procedure ensures that the paths leading to higher-quality solutions are strengthened, increasing the probability that the ants will follow these paths in future iterations of the algorithm.

The optimization of the hybrid microgrid was implemented in Python 3.12.7 using pandas for data manipulation, *deap* for GA, *networkx* for ACO, and *itertools* for exhaustive search. A base case (evaluated system) with three 550 W solar panels, a 1 kW wind turbine, and a 3 kWh BESS was created (Table 1), and the data detailed in Figure 3 were structured. The simulation was defined in the *simulate configuration()* function, which calculates EENS, LOLP, and LPSP using vectorized operations in *numpy* to improve performance. In GA, the individuals represent generation and storage configurations optimized by tournament selection *(tools.selTournament())*, blend crossover (*cxBlend*, $\alpha = 0.5$), and Gaussian mutation (*mutGaussian(mu = 0, sigma = 1)*). The evolutionary process runs 20 generations with an

initial population of 50 individuals and evaluates the *fitness function evaluate()*, which calls *simulate_configuration()* and minimizes the EENS.

For the ACO, a graph was modeled in *networkx*, where each node represents a configuration, and the pheromones on the edges are updated according to the quality of the solution found. One hundred iterations were run, generating random solutions with *random.uniform()* and reinforcing the best routes with an evaporation factor of 10%. In the exhaustive search, *itertools.product()* generated all possible combinations within a given range, and for each of them the *simulate_configuration()* function was evaluated. The results were plotted using *matplotlib*.

3. Results

3.1. Microgrid Evaluation and Diagnosis

3.1.1. Description of Initial Configurations

Table 2 shows the technical capabilities and costs of the components of the evaluated system, which includes photovoltaic (PV) panels, a wind turbine, and a BESS. The photovoltaic system has a generating capacity of 3.30 kW (6 panels of 550 W), the wind turbine has a capacity of 1 kW, and the battery storage system has a capacity of 3 kWh. In terms of cost, the photovoltaic system costs USD 3250, the wind turbine costs USD 1200, and the battery system costs USD 1500, which means that the total cost of the complete system is USD 5950.

Table 2. The capability and costs of the system are being evaluated.

Category	Capacity (kW/kWh)	Cost (USD)
PV	3.25	3250
Wind	1	1200
BESS	3	1500

3.1.2. Reliability Assessment

Figure 4 shows the analysis of the reliability metrics of the microgrid, which consists of a 3.25 kW photovoltaic system, a 1 kW wind turbine, and a 3 kWh BESS. The LOLP (loss of load probability) indicator has a value of 0.22, representing a 22% probability of load loss in the system. The LPSP (probability of power supply loss) indicator has a value of 0.26, reflecting a 26% probability of power supply loss. Finally, the availability of the system is 77%, meaning that it operates correctly 77% of the time.
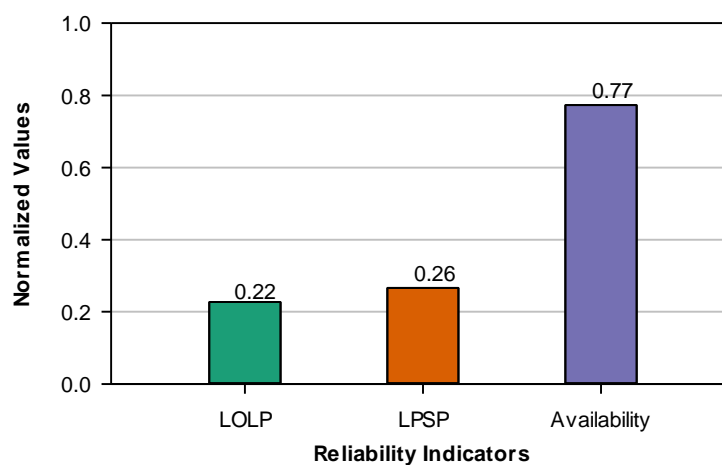

Figure 4. Residential Microgrid reliability indicators evaluated.

3.1.3. Dynamic Performance of the Microgrid

Analysis of the Average Daily Load (ADL) throughout the year shows fluctuations between 0.2 and 0.8, as shown in Figure 5. During the first quarter, the ADL remains at low or moderate levels, possibly due to lower generation or higher consumption. Between April and September, the average SOC increases and reaches maximum values at different times, which could be related to a greater availability of renewable energy. However, during the same period, abrupt drops in SOC are observed, indicating variability in generation or consumption. From October to December, the average SOC decreases again, possibly due to limitations in generation or an increase in demand. The daily variability of SOC shows that storage management is not constant and is due to differences in renewable energy generation or consumption profiles.
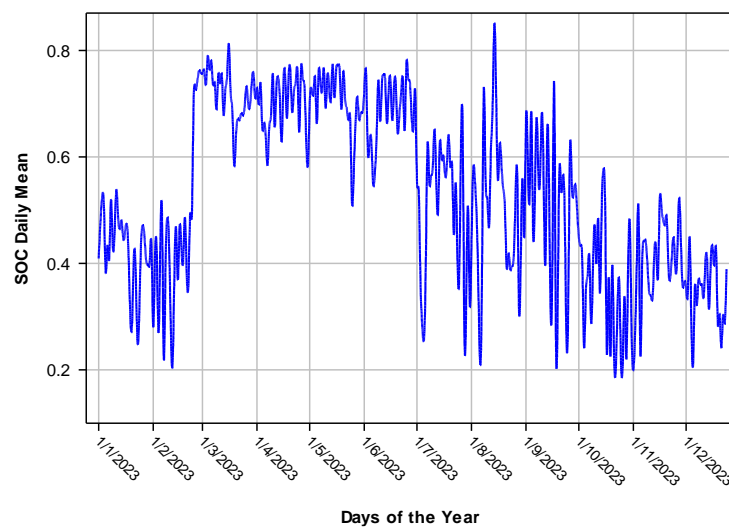

Figure 5. Daily SOC means for the evaluated microgrid.

Similarly, Figure 6 shows the balance between charge (P_{chg}) and discharge (P_{dchg}) in the monthly analysis, with similar average values throughout the year. However, seasonal variations can be observed. The average charge is higher in February and October, while the average discharge increases in the months of high demand, such as July and November. The average monthly SOC remains within a range of 0.4 to 0.6, indicating stable operation, although periods of lower storage levels are identified.
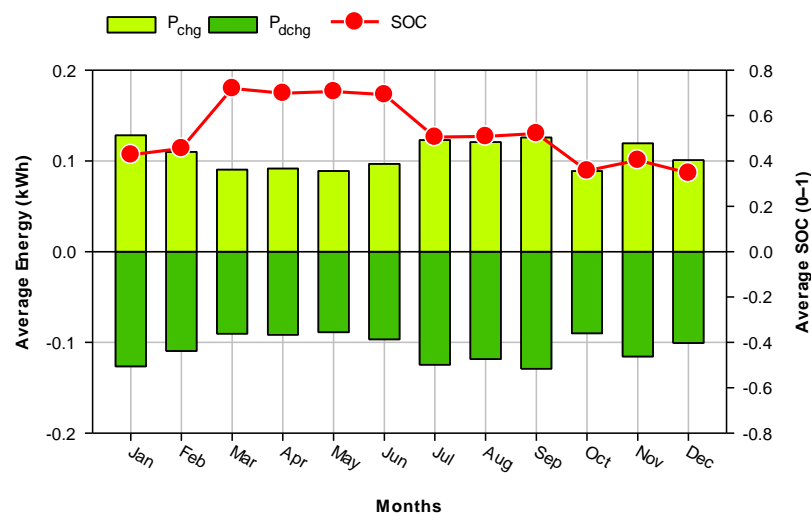

Figure 6. Monthly means of SOC, charging (P_{chg}), and discharging (P_{dchg}) of the BESS.

On the other hand, the hourly analysis confirms these observations as it shows an average of P_{chg} and P_{dchg} of 0.107, confirming the balance of the system. However, the standard deviation of P_{chg} (0.237) is greater than that of P_{dchg} (0.177), indicating more pronounced load variations. The average hourly SOC (0.532) is consistent with the monthly results, but its standard deviation (0.259) and 25th percentile (0.221) indicate that the battery is operating at low charge levels for a quarter of the time. The records show the overall stability of the system but also highlight the need to optimize its operation. The fluctuations in P_{chg} and the periods of low SOC (minimum) show the importance of identifying this inactivity in the charge and, therefore, in the discharge, as well as stabilizing the storage level.

Figure 7 shows the relationship between energy production and the average monthly demand for the photovoltaic–wind hybrid system. First, the average monthly demand of the house, represented by D(t), differs from the total combined production of photovoltaic energy (P_{pv}) and wind energy (P_{wind}) in several months of the year. This indicates that the system cannot fully satisfy the energy needs of the house in all the periods analyzed.
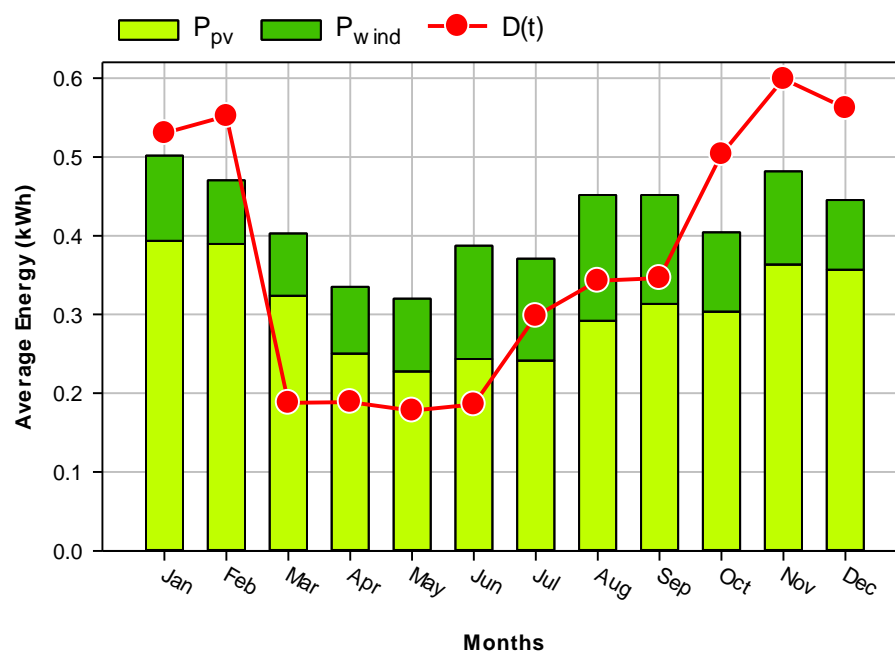

Figure 7. Mean monthly photovoltaic and wind energy compared to household consumption.

Most of the generation comes from photovoltaic energy, which is in line with the higher installed capacity of the photovoltaic system (3.25 kW) compared to the wind turbine (1 kW). Wind power, although less significant in absolute terms, has a more constant contribution throughout the year. Photovoltaic generation, on the other hand, shows greater seasonal variability, with lower levels in the winter months (December, January, and February), possibly due to the reduction in solar radiation characteristic of this period.

On the other hand, the average monthly demand reaches significant peaks in the months of February and November, related to specific consumption patterns, such as the use of heating systems or appliances with high energy demand. From May to August, there is a closer relationship between total production and demand, indicating a better balance between energy supply and demand during this period.

3.1.4. Limitations and Improvement Points of the Microgrid

The evaluated system has significant limitations in terms of reliability and operational capacity. The system has an availability of 77%, which means that it is not operational

for 23% of the time, which affects the continuity of supply. In addition, the LOLP (0.22) and LPSP (0.26) indicators demonstrate a significant probability of load loss and power interruption. The limited capacity of the storage system is reflected in an average state of charge that fluctuates between 0.4 and 0.6, reaching a minimum of 0.2 in certain critical periods and during hours when there is no charging or discharging, with an average SOC of 0.423 and a 25th percentile of 0.200 (lower limit of the SOC), indicating an insufficiency to cover energy needs.

The generation of the system is also insufficient in the months of lower photovoltaic availability, especially in winter, when it is unable to meet the average demand. Photovoltaic generation has a high seasonal variability, while wind turbines, although more constant, have a limited capacity to make up the deficit. In addition, there are significant fluctuations in charging and discharging power, with greater variability in charging (standard deviation of 0.237 compared to 0.177 in discharging), which affects the stability of the system. These conditions result in high costs for energy not supplied and a constant imbalance between energy supply and demand, especially in the months of high demand, such as February and November.

3.2. Optimization of the Microgrid

3.2.1. Impact of Optimization on Reliability and Cost

Table 3 presents the impact of optimization on the reliability and cost of the residential microgrid system. The evaluation of the current (base) system shows that the base configuration has limitations in terms of reliability and availability, indicating a high probability of load loss and power outages. The availability of the system indicates frequent interruptions in the power supply. Optimization using genetic algorithms made it possible to increase the photovoltaic capacity to 4.25 kW and the battery to 4 kWh, reduce LOLP to 0.11 and LPSP to 0.164, and improve system availability to 89%. However, the cost of the GA-optimized system is USD 7450. On the other hand, optimization with ant colony algorithms increased the wind capacity to 1.5 kW and the battery to 4 kWh, achieving the same reliability as GA, but at a lower cost of USD 7050. The configuration obtained through an exhaustive search approach increased reliability, with LOLP values of 0.081 and LPSP of 0.128, as well as 91% availability, but its cost was higher, USD 10,150.

Table 3. Impact of optimization on the reliability and cost of the residential microgrid system.

Item	PV (kW)	Wind (kW)	BESS (kWh)	LOLP	LPSP	Availability	Total Cost (USD)
Base	3.25	1	3	0.227	0.266	0.77	5950
GA	4.25	1	4	0.11	0.164	0.89	7450
ACO	3.25	1.5	4	0.11	0.164	0.89	7050
Exhaustive	5.25	2	5	0.081	0.128	0.91	10,150

Based on this, the results show that the ACO-based optimization achieves a balance between reliability and cost and provides significant improvements in system stability without an excessive increase in investment. The GA-based configuration also improves reliability, although its cost is slightly higher. The exhaustive search presents an improvement in terms of reliability, but its high cost limits its feasibility.

Table 4 shows the temporal and spatial complexity of simulation methods in an autonomous energy system. The GA methods have a complexity of O(8592) and O(n), while ACO and Exhaustive increase the time to O(17,184) and O(34,368), and the memory usage to O(2n) and O(4n), respectively. ACO's processing increases but remains manageable, while Exhaustive is the most expensive in terms of time and memory. GA is the most efficient option for large amounts of data.

Table 4. Method complexity estimation.

Item	Time Complexity	Space Complexity
GA	O(8592)	O(n)
ACO	O(17,184)	O(2n)
Exhaustive	O(34,368)	O(4n)

3.2.2. Dynamic Stability of the Microgrid

Figure 8 shows the evolution of the monthly energy balance (Mean Energy Balance, kWh) when considering different strategies to optimize renewable energy generation using metaheuristic techniques. The configurations evaluated are base (3.25 PV, 1 Wind), corresponding to the initial microgrid; GA (4.25 PV, 1 Wind), optimized with GA; ACO (3.25 PV, 1.5 Wind), optimized with ACO; and Exhaustive (5.25 PV, 2 Wind), characterized by the highest installed capacity obtained through exhaustive search. The monthly energy demand, represented as D(t), shows seasonal variations, with peaks recorded in January, February, October, and December.
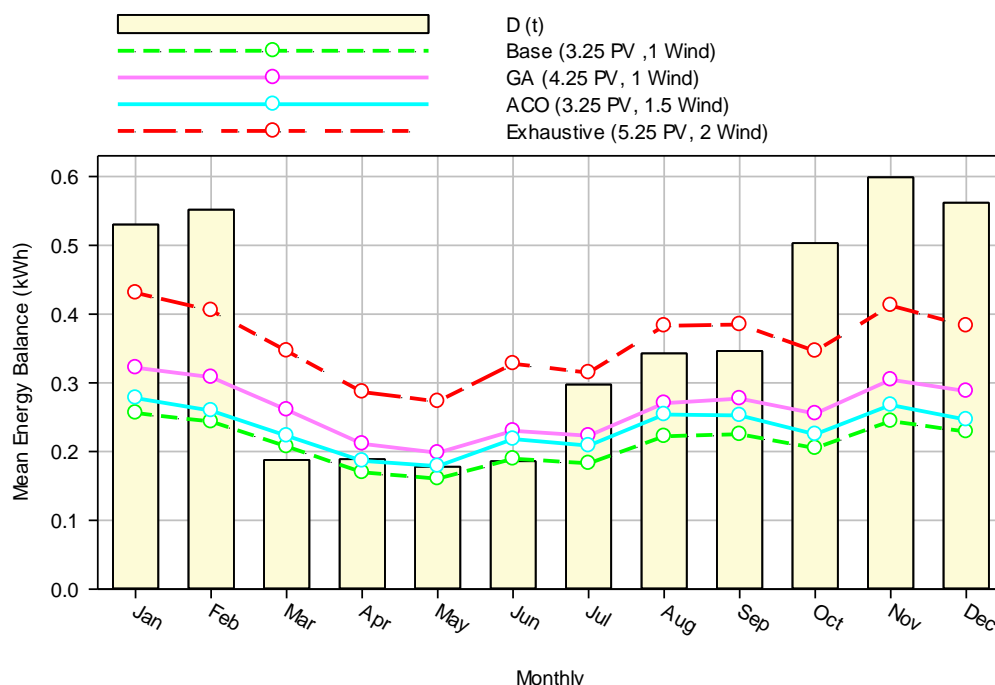

Figure 8. Mean monthly energy balance (kWh).

During the months of lower demand (April to July), all the optimized configurations come closer to satisfying the demand, reducing the discrepancies between generation and consumption. The base configuration presents the lowest energy balance in all the months analyzed, so it is not enough to satisfy the demand in the periods of highest consumption, which highlights the need to increase the installed capacity. On the contrary, the optimized configurations GA and ACO show a significant improvement in the stability of the energy balance throughout the year. In particular, the ACO configuration stands out from July to September, as it achieves a higher energy balance thanks to a more efficient distribution between wind and photovoltaic generation.

The Exhaustive configuration, with the highest installed capacity, generates a slightly higher energy balance in all the months evaluated. However, this improvement in generation is associated with a significant increase in investment costs, which could limit its economic viability. On the other hand, the GA and ACO configurations are more efficient

alternatives than the base configurations, as they reduce the energy deficit in periods of high demand without implying a significant increase in installed capacity.

In terms of efficiency, the ACO configuration stands out as the best alternative among the optimized options, as it maximizes the combination of wind and photovoltaic generation with a more balanced use of available resources. However, if the main objective is to guarantee energy supply without economic constraints, the Exhaustive configuration offers the most robust solution, although its implementation requires a detailed evaluation of the associated costs.

3.2.3. State of Charge (SOC) Analysis

The analysis of the Annual Daily Mean (ADM) of the SOC in the evaluated configurations shows that greater storage system stability is achieved when optimization strategies are implemented, as shown in Figure 9. The Base configuration has the lowest average SOC value (0.6902), while the GA and ACO configurations increase it to 0.7201, and the Exhaustive configuration reaches a slightly higher value of 0.7427. These differences reflect the direct impact of storage capacity optimization on system reliability.
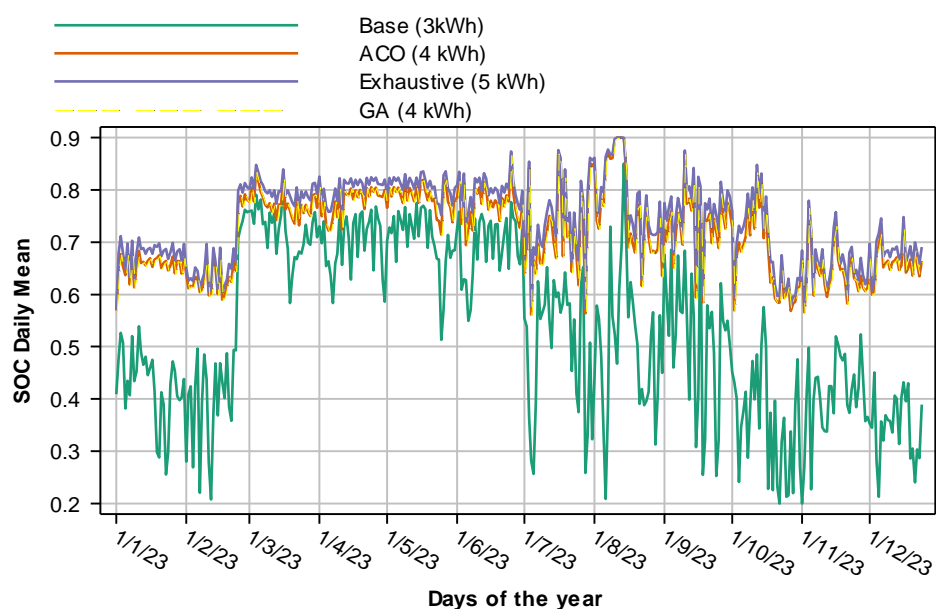

Figure 9. Annuals mean daily SOC of the optimized microgrid configurations.

From a sizing perspective, battery capacity is critical to SOC stability. The base configuration operates with a battery capacity of 3 kWh, which generates a LOLP (loss of load probability) of 0.227, indicating a high probability of power failure. In contrast, the optimized GA and ACO configurations increase the storage capacity to 4 kWh, reducing the LOLP to 0.11 and improving energy availability from 77% to 89%. The Exhaustive configuration, with 5 kWh of battery capacity, slightly reduces the LOLP to 0.081, ensuring 91% availability to meet demand.

The impact of installed capacity on energy reliability is also reflected in the LPSP, which decreases as generation is optimized. The base configuration has an LPSP of 0.266, indicating the highest rate of outages. The GA and ACO configurations reduce this to 0.164, while the Exhaustive configuration achieves the lowest outage probability with an LPSP of 0.128. From an economic perspective, capital costs increase with installed capacity. The base configuration has the lowest total cost of USD 5950, while the optimized GA and ACO configurations require investments of USD 7450 and USD 7050, respectively. The full

configuration, with the highest generation and storage capacity, has a cost of USD 10,150, reflecting the trade-off between reliability and implementation cost.

Analysis of the SOC and reliability metrics suggests that the GA and ACO configurations improve storage and reduce the energy deficit without an excessive increase in investment. In particular, the ACO configuration distributes wind and photovoltaic generation more efficiently, resulting in a better energy balance during periods of lower solar irradiation. The full configuration, while maximizing energy reliability, must be evaluated for economic viability due to high implementation costs. The annual average hourly SOC complements the daily results and provides information on the charge and discharge dynamics of the storage system, as shown in Figure 10. A progressive decrease in SOC can be observed from midnight to the early hours of the morning, reaching its minimum value between 10:00 and 12:00. Subsequently, the SOC recovers from noon due to the increase in photovoltaic generation.
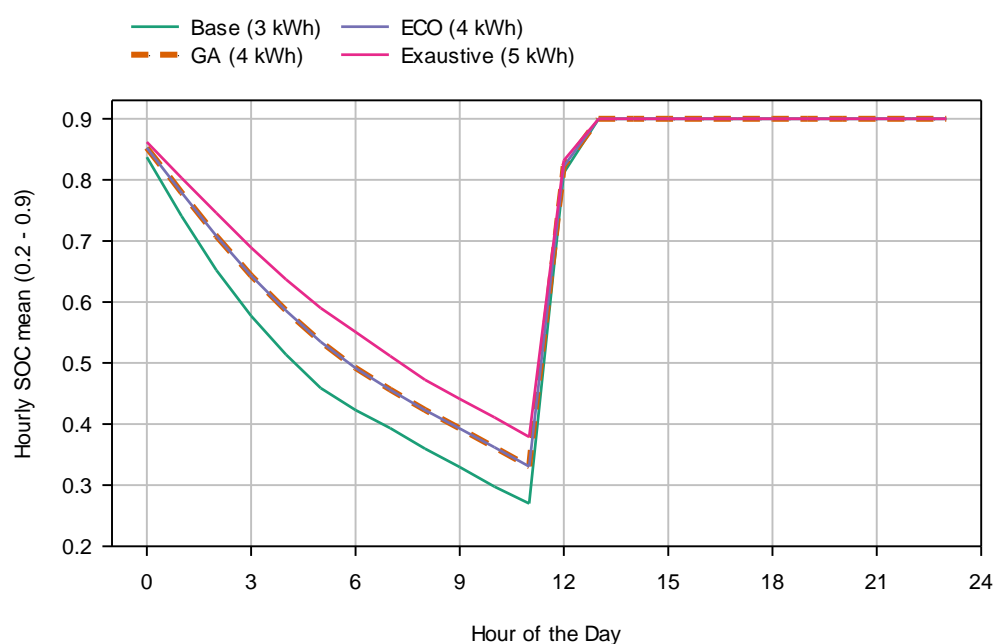

Figure 10. Annual average hourly SOC for optimized configurations.

The hourly behavior shows that the base configuration has the greatest variability and the most pronounced drop in SOC during the early hours of the morning, with minimum values close to 30% load, confirming its insufficiency to cover nighttime demand without incurring an energy deficit. The GA and ACO configurations show greater stability, with minimum values between 35 and 40%, indicating that increasing the battery capacity and optimizing the generation reduces the energy deficit at night. The comprehensive configuration shows the most robust behavior, with the least decrease in SOC and values that never fall below 45% at any time of the day.

The relationship between daily and hourly analysis confirms that the reliability of the system increases as the storage capacity increases. The greater stability in the GA and ACO configurations indicates that optimizing generation and battery sizing are effective strategies for reducing the energy deficit, especially in the early morning hours. The Exhaustive configuration, while providing the greatest stability, is associated with high costs that may affect its viability in terms of implementation.

4. Discussion

The reliability analysis of the evaluated microgrid shows that the base configuration is deficient in power continuity, with LOLP and LPSP values of 22.7% and 26.6%, respectively. The initial renewable energy generation and storage capacity are not sufficient to always meet the demand, which affects the stability of the system. Therefore, the availability of the system is 77%.

Optimization using metaheuristic algorithms (GA and ACO) improved the reliability of the system. The GA-optimized configuration increased the photovoltaic capacity to 4.25 kW and the storage capacity to 4 kWh, reducing the LOLP to 11% and the LPSP to 16.4%, with an availability of 89%. This result is consistent with other recent work that has succeeded in reducing the LPSP and improving the reliability of the hybrid photovoltaic/wind/fuel cell/battery renewable energy system, subject to certain constraints on the energy flow and state of charge of the battery [17]. The results of this study showed that the GA optimization algorithm improved the energy flow and made it possible to keep the battery state of charge within the safe range of 20% to 95%. Regarding the proposed system, the authors emphasize that its dependence on the main grid was reduced to 5.80%, in contrast to the initial installation, which still required 15% grid support [17]. In contrast, in this work, it was possible to reduce this dependence from 22.7% to 11% using the GA optimization algorithm, which sought to balance the reliability of the system with the costs associated with the installation of the microgrid.

Similarly, optimization with ACO increased the wind capacity to 1.5 kW and the battery capacity to 4 kWh, achieving reliability like GA at a lower cost. These results are consistent with other studies that used ACO as part of a two-stage stochastic approach to optimize microgrid operation [34]. That is, for building consumption, the Euclidean distance was 4.2 kW in the best case and 16.54 kW in the worst case, indicating that the ACO method generated scenarios that were representative of actual demand. Other studies report that the ACO algorithm outperformed the Gray Wolf Optimizer (GWO), Bat Algorithm (BSA), and Whale Optimization Algorithm (WOA) in optimizing a photovoltaic microgrid with energy storage, demonstrating higher efficiency and accuracy [19].

The configuration obtained through an exhaustive search achieved lower LOLP and LPSP values, with an availability of 91%, although the cost was higher. In addition, all possible combinations were explored without applying heuristics or search space reduction strategies, resulting in extensive computational time. In this context, ACO shows a better reliability/cost ratio, while GA improves reliability at an additional cost. Exhaustive search achieves the best reliability but at a very high cost. Similarly, the SOC analysis shows that the baseline configuration has greater variability in storage availability, with an average SOC of 0.69, and drops below 30% in critical hours. The configurations optimized with GA and ACO increase the average SOC to 0.72 and 0.74, respectively, improving the stability of the energy storage.

In terms of dynamic stability, the energy balance analysis shows that the optimized configurations reduce the discrepancies between generation and consumption in the months of lower demand. The ACO configuration presents a better balance between wind and photovoltaic generation, while the GA configuration depends more on photovoltaic generation. The configuration obtained by exhaustive search guarantees a stable supply, but its cost is high.

The limitations of the study are that it uses data from a single microgrid in a specific location. Future studies should evaluate it with other types of data and locations. However, the selection of a single microgrid allows for strict control of the variables, which facilitates an accurate evaluation of the phenomenon studied. The methodology used guarantees

the reliability of the results within the analyzed context, serving as a basis for subsequent studies that expand the sample and validate the results in more diverse scenarios.

5. Conclusions

The objective of this article was to analyze and optimize the reliability of an autonomous residential microgrid based on solar PV, wind, and BESS using GA and ACO. The evaluation focused on LOLP, availability, and associated costs.

The initial configuration of the microgrid showed limitations in terms of reliability, with an availability of 77% and high values of LOLP (22.7%) and LPSP (26.6%), indicating a high probability of power outages.

Optimization using metaheuristic algorithms significantly improved system reliability, reducing LOLP and LPSP to 11% and 16.4%, respectively, and increasing availability to 89%.

The configuration optimized with ACO achieved a balance between reliability and cost, while GA improved reliability at a slightly higher cost. The exhaustive search provided the highest reliability, but at a significantly higher cost.

The State of Charge (SOC) analysis showed that the optimized configurations reduced the fluctuations of the energy storage, which guarantees a higher stability of the supply.

The energy balance evaluation showed that the optimized configurations reduced the imbalance between generation and consumption during the months of lower demand. In addition, the ACO distributed wind and photovoltaic generation more efficiently.

Therefore, optimization using metaheuristic algorithms is presented as an effective strategy for improving the reliability of autonomous microgrids, as it allows for achieving a balance between availability, a reduction in energy deficit, and implementation costs.

Author Contributions: Conceptualization, methodology, software, formal analysis, investigation, resources, data curation, writing—original draft preparation, and visualization: E.Z.-P. Validation: E.Z.-P. and R.S. Writing—review and editing, supervision, and project administration: R.S. All authors have read and agreed to the published version of the manuscript.

Data Availability Statement: The data supporting the findings of this study are not publicly available due to confidentiality restrictions.

Conflicts of Interest: The authors declare no conflicts of interest.

References

1. Kay Lup, A.N.; Soni, V.; Keenan, B.; Son, J.; Taghartapeh, M.R.; Morato, M.M.; Poya, Y.; Montañés, R.M. Sustainable Energy Technologies for the Global South: Challenges and Solutions toward Achieving SDG 7. *Environ. Sci. Adv.* **2023**, *2*, 570–585. [CrossRef]
2. Zarate-Perez, E.; Sebastián, R. Autonomy Evaluation Model for a Photovoltaic Residential Microgrid with a Battery Storage System. *Energy Rep.* **2022**, *8*, 653–664. [CrossRef]
3. Dong, L.; Lin, H.; Qiao, J.; Zhang, T.; Zhang, S.; Pu, T. A Coordinated Active and Reactive Power Optimization Approach for Multi-Microgrids Connected to Distribution Networks with Multi-Actor-Attention-Critic Deep Reinforcement Learning. *Appl. Energy* **2024**, *373*, 123870. [CrossRef]
4. Kontani, R.; Tanaka, K. Integrating Variable Renewable Energy and Diverse Flexibilities: Supplying Carbon-Free Energy from a Wind Turbine to a Data Center. *Urban Clim.* **2024**, *54*, 101843. [CrossRef]
5. Medghalchi, Z.; Taylan, O. A Novel Hybrid Optimization Framework for Sizing Renewable Energy Systems Integrated with Energy Storage Systems with Solar Photovoltaics, Wind, Battery and Electrolyzer-Fuel Cell. *Energy Convers. Manag.* **2023**, *294*, 117594. [CrossRef]
6. Barva, A.V.; Joshi, S. Empowering Hybrid Renewable Energy Systems with BESS for Self-Consumption and Self-Sufficiency. *J. Energy Storage* **2024**, *82*, 110561. [CrossRef]

7. Hussain, A.; Huseynova, A.; Hakimova, Y.; Nassani, A.A.; Bo, B. Energy Efficiency and Emission Flexibility: Management and Economic Insights for Renewable Energy Integration. *Energy Strateg. Rev.* **2025**, *57*, 101631. [CrossRef]

8. Zou, Y.; Čepin, M. Loss of Load Probability for Power Systems Based on Renewable Sources. *Reliab. Eng. Syst. Saf.* **2024**, *247*, 110136. [CrossRef]

9. Mahesh, A.; Sandhu, K.S. Hybrid Wind/Photovoltaic Energy System Developments: Critical Review and Findings. *Renew. Sustain. Energy Rev.* **2015**, *52*, 1135–1147. [CrossRef]

10. Emrani, A.; Berrada, A. A Comprehensive Review on Techno-Economic Assessment of Hybrid Energy Storage Systems Integrated with Renewable Energy. *J. Energy Storage* **2024**, *84*, 111010. [CrossRef]

11. Motamedisedeh, O.; Omrani, S.; Karim, A.; Drogemuller, R.; Walker, G. A Comprehensive Review of Optimum Integration of Photovoltaic-Based Energy Systems. *Renew. Sustain. Energy Rev.* **2025**, *207*, 114935. [CrossRef]

12. Reinert, C.; Nolzen, N.; Frohmann, J.; Tillmanns, D.; Bardow, A. Design of Low-Carbon Multi-Energy Systems in the SecMOD Framework by Combining MILP Optimization and Life-Cycle Assessment. *Comput. Chem. Eng.* **2023**, *172*, 108176. [CrossRef]

13. Zhou, D.; Liu, Y.; Wang, X.; Wang, F.; Jia, Y. Research Progress of Photovoltaic Power Prediction Technology Based on Artificial Intelligence Methods. *Energy Eng.* **2024**, *121*, 3573–3616. [CrossRef]

14. Lu, P.; Zhang, N.; Ye, L.; Du, E.; Kang, C. Advances in Model Predictive Control for Large-Scale Wind Power Integration in Power Systems. *Adv. Appl. Energy* **2024**, *14*, 100177. [CrossRef]

15. Modu, B.; Abdullah, M.P.; Bukar, A.L.; Hamza, M.F. A Systematic Review of Hybrid Renewable Energy Systems with Hydrogen Storage: Sizing, Optimization, and Energy Management Strategy. *Int. J. Hydrogen Energy* **2023**, *48*, 38354–38373. [CrossRef]

16. Rawat, T.; Singh, J.; Sharma, S.; Niazi, K.R. Stochastic Multi-Objective Bi-Level Optimization Model for Operation of Active Distribution System with Demand Response. In Proceedings of the 2022 22nd National Power Systems Conference (NPSC), New Delhi, India, 17–19 December 2022; pp. 12–17. [CrossRef]

17. Agoundedemba, M.; Kim, C.K.; Kim, H.G.; Nyenge, R.; Musila, N. Modelling and Optimization of Microgrid with Combined Genetic Algorithm and Model Predictive Control of PV/Wind/FC/Battery Energy Systems. *Energy Rep.* **2025**, *13*, 238–255. [CrossRef]

18. Marzband, M.; Yousefnejad, E.; Sumper, A.; Domínguez-García, J.L. Real Time Experimental Implementation of Optimum Energy Management System in Standalone Microgrid by Using Multi-Layer Ant Colony Optimization. *Int. J. Electr. Power Energy Syst.* **2016**, *75*, 265–274. [CrossRef]

19. Li, S.; Deng, N.; Lee, X.; Yan, S.; Chen, C. Optimal Configuration of Photovoltaic Microgrid with Improved Ant Colony Dynamic Programming. *J. Energy Storage* **2024**, *83*, 110714. [CrossRef]

20. Sengupta, M.; Xie, Y.; Lopez, A.; Habte, A.; Maclaurin, G.; Shelby, J. The National Solar Radiation Data Base (NSRDB). *Renew. Sustain. Energy Rev.* **2018**, *89*, 51–60. [CrossRef]

21. Imad Hazim, H.; Azmi Baharin, K.; Kim Gan, C.; Sabry, A.H. Techno-Economic Optimization of Photovoltaic (PV)-Inverter Power Sizing Ratio for Grid-Connected PV Systems. *Results Eng.* **2024**, *23*, 102580. [CrossRef]

22. Xia, S.; Chan, K.W.; Luo, X.; Bu, S.; Ding, Z.; Zhou, B. Optimal Sizing of Energy Storage System and Its Cost-Benefit Analysis for Power Grid Planning with Intermittent Wind Generation. *Renew. Energy* **2018**, *122*, 472–486. [CrossRef]

23. Abed, M.; Reddy, B.A.; Jyothsna, T.R.; Mohammed, N. Optimal Sizing and Performance Assessment of Stand-Alone PV Systems Using Optimum Hybrid Sizing Strategy. *Results Eng.* **2025**, *25*, 103793. [CrossRef]

24. Cai, C.; Zhang, L.; Lai, G.; Zhou, J.; Zhou, L.; Qin, Y.; Tang, Z. Optimal Sizing and Cost-Benefit Assessment of Stand-Alone Microgrids with Different Energy Storage Considering Dynamic Avoided GHG Emissions. *J. Energy Storage* **2025**, *109*, 115128. [CrossRef]

25. Kuo, T.C.; Pham, T.T.; Bui, D.M.; Le, P.D.; Van, T.L.; Huang, P.T. Reliability Evaluation of an Aggregate Power Conversion Unit in the Off-Grid PV-Battery-Based DC Microgrid from Local Energy Communities under Dynamic and Transient Operation. *Energy Rep.* **2022**, *8*, 5688–5726. [CrossRef]

26. Zarate-Perez, E.; Santos-Mejía, C.; Sebastián, R. Reliability of Autonomous Solar-Wind Microgrids with Battery Energy Storage System Applied in the Residential Sector. *Energy Rep.* **2023**, *9*, 172–183. [CrossRef]

27. Lou, J.; Cao, H.; Meng, X.; Wang, Y.; Wang, J.; Chen, L.; Sun, L.; Wang, M. Power Load Analysis and Configuration Optimization of Solar Thermal-PV Hybrid Microgrid Based on Building. *Energy* **2024**, *289*, 129963. [CrossRef]

28. Ould Bilal, B.; Sambou, V.; Ndiaye, P.A.; Kébé, C.M.F.; Ndongo, M. Optimal Design of a Hybrid Solar–Wind-Battery System Using the Minimization of the Annualized Cost System and the Minimization of the Loss of Power Supply Probability (LPSP). *Renew. Energy* **2010**, *35*, 2388–2390. [CrossRef]

29. Ullah, F.; Hasrat, K.; Iqbal, S.; Kumar, S.; Wang, S.; Mu, M.; Lu, W. Evaluating the Global Warming Potential of a 4.6 KWp Solar PV System in Karak-KPK: A Life Cycle Assessment. *Appl. Therm. Eng.* **2025**, *266*, 125790. [CrossRef]

30. Domashova, J.V.; Emtseva, S.S.; Fail, V.S.; Gridin, A.S. Selecting an Optimal Architecture of Neural Network Using Genetic Algorithm. *Procedia Comput. Sci.* **2021**, *190*, 263–273. [CrossRef]

31. Inomoto, R.; Filho, A.J.S.; Monteiro, J.R.; da Costa, E.C.M. Genetic Algorithm Based Tuning of Sliding Mode Controllers for a Boost Converter of PV System Using Internet of Things Environment. *Results Control Optim.* **2024**, *14*, 100389. [CrossRef]
32. Alamir, N.; Kamel, S.; Abdelkader, S.M. Stochastic Multi-Layer Optimization for Cooperative Multi-Microgrid Systems with Hydrogen Storage and Demand Response. *Int. J. Hydrogen Energy* **2025**, *100*, 688–703. [CrossRef]
33. Kolamroudi, M.K.; Ilkan, M.; Egelioglu, F.; Safaei, B. Feature Selection by Ant Colony Optimization and Experimental Assessment Analysis of PV Panel by Reflection of Mirrors Perpendicularly. *Renew. Energy* **2023**, *218*, 119238. [CrossRef]
34. Valderrama, D.F.; Ferro, G.; Guerrero Alonso, J.I.; De Mora, C.L.; Parodi, L.; Robba, M. Smart Grid Stochastic Optimization with Ant Colony-Based Scenario Generation. *IFAC-PapersOnLine* **2024**, *58*, 112–117. [CrossRef]